Pflugers Arch - Eur J Physiol (2007) 455:223–239
DOI 10.1007/s00424-007-0281-8

ACID-BASE REGULATION

HCO_3^--dependent pH_i recovery and overacidification induced by NH_4^+ pulse in rat lung alveolar type II cells: HCO_3^--dependent NH_3 excretion from lungs?

Sachiko Tokuda · Chikao Shimamoto · Hideyo Yoshida · Hitoshi Murao · Gen-ichi Kishima · Shigenori Ito · Takahiro Kubota · Toshiaki Hanafusa · Tohru Sugimoto · Naomi Niisato · Yoshinori Marunaka · Takashi Nakahari

Received: 13 April 2007 / Revised: 13 April 2007 / Accepted: 19 April 2007 / Published online: 12 June 2007

Abstract Intracellular pH (pH_i) after the NH_4^+ pulse addition and its removal were measured in isolated alveolar type II cells (ATII cells) using BCECF fluorescence. In the absence of HCO_3^-, the NH_4^+ pulse addition increased pH_i (alkali jump) and its removal decreased pH_i (acid jump) to the control level (no overacidification). This pH_i change was induced by reaction 1 $\left(NH_3 + H^+ \leftrightarrow NH_4^+\right)$. However, in the presence of HCO_3^-, the NH_4^+ pulse removal decreased pH_i (acid jump) with overacidification. The extent of overacidification was decreased by acetazolamide (a carbonic anhydrase inhibitor), bumetanide (an inhibitor of $Na^+/K^+/2Cl^-$ cotransporter [NKCC]), and NPPB (an inhibitor of Cl^- channel). The NH_4^+ pulse addition led to the accumulation of NH_4^+ in ATII cells via reaction 1 and NKCC, and the NH_4^+ pulse removal induced reaction 2 $\left(NH_4^+ + HCO_3^- \rightarrow NH_3 + H^+ + HCO_3^-\right)$ in addition to the reversal of reaction 1. Thus, NH_4^+ that entered via NKCC reacts with HCO_3^- (reaction 2) to produce H^+, which induces overacidification in the acid jump. After the overacidification, the pH_i recovery consisted of a rapid recovery (first phase) followed by a slow recovery (second phase). The first phase was inhibited by NPPB, glybenclamide, amiloride, and an Na^+-free solution, and the second phase was inhibited by DIDS, MIA, and an Na^+-free solution. Both phases were accelerated by a high extracellular HCO_3^- concentration. These observations indicate that the first phase was induced by HCO_3^- entry via Cl^- channels coupled with Na^+ channels activities, and that the second phase was induced by H^+ extrusion via Na^+/H^+ exchanger and by HCO_3^- entry via $Na^+ - HCO_3^-$ cotransporter. Thus, in ATII cells, HCO_3^- entry via Cl^- channels is essential for recovering pH_i after overacidification during the acid jump and for removing NH_4^+ that entered via NKCC from ATII cells, suggesting HCO_3^--dependent NH_3 excretion from lungs.

S. Tokuda · C. Shimamoto · H. Yoshida · H. Murao · G. Kishima · S. Ito · T. Kubota · T. Hanafusa · Y. Marunaka · T. Nakahari
Central Research Laboratory (Nakahari Project), Osaka Medical College, 2-7 Daigakucho, Takatsuki 569-8686, Japan

H. Yoshida · T. Kubota · T. Nakahari (✉)
Department of Physiology, Osaka Medical College, 2-7 Daigakucho, Takatsuki 569-8686, Japan
e-mail: takan@art.osaka-med.ac.jp

S. Ito
Department of Chemistry, Osaka Medical College, 2-7 Daigakucho, Takatsuki 569-8686, Japan

C. Shimamoto · H. Murao · G. Kishima · T. Hanafusa
Department of Internal Medicine, Osaka Medical College, 2-7 Daigakucho, Takatsuki 569-8686, Japan

S. Tokuda · N. Niisato · Y. Marunaka
Department of Molecular Cell Physiology, Graduate School of Medical Science, Kyoto Prefectural University of Medicine, Kyoto, Japan

S. Tokuda · T. Sugimoto
Department of Pediatrics, Graduate School of Medical Science, Kyoto Prefectural University of Medicine, Kyoto, Japan

Keywords Cl^- channels · Carbonic anhydrase · $Na^+/K^+/2Cl^-$ cotransport

Introduction

The NH_4^+ pulse method is used to investigate intracellular pH (pH_i) regulation in many cell types including alveolar type II (ATII) cells [1–4]. The NH_4^+ pulse addition increases pH_i (alkali jump) by reaction 1, in which NH_3 that entered reacts with H^+ to produce NH_4^+:

$$NH_3 + H^+ \leftrightarrow NH_4^+. \quad (1)$$

This increases pH_i because NH_4^+ solution contains small amounts of NH_3 (pK_a=9.25, NH_4^+/NH_3 = 25 mM/0.35 mM at pH=7.4). Therefore, the NH_4^+ pulse addition induces NH_4^+ accumulation in cells. In contrast, its removal induces the reconversion from NH_4^+ to NH_3 and H^+ (the reversal of reaction 1); consequently, pH_i decreases (acid jump). The reversal of reaction 1 appears to return pH_i to the control level before the NH_4^+ pulse addition. However, in many cell types, NH_4^+ pulse removal induces an overacidification during the acid jump [1, 2]. The overacidification is explained as follows: NH_4^+ that entered via the $Na^+/K^+(NH_4^+)/2Cl^-$ cotransporter (NKCC) is also converted to H^+ and NH_3 (the reversal of reaction 1) after the NH_4^+ pulse removal [2, 5–7].

Under the HCO_3^--containing condition, the NH_4^+ pulse addition induces an alkali jump, and the NH_4^+ pulse removal induces an acid jump with overacidification in ATII cells. We also carried out the experiments under the HCO_3^--free condition. However, under the HCO_3^--free condition, the NH_4^+ pulse removal induced no overacidification during the acid jump, and pH_i immediately returned to the control level before the NH_4^+ pulse addition; although NH_4^+ pulse addition induced a similar alkali jump [3]. The overacidification during the acid jump appears to be a HCO_3^--dependent process. In the presence of HCO_3^-, reaction 2 may also occur in addition to reaction 1.

$$NH_4^+ + HCO_3^- \leftrightarrow NH_3 + H^+ + HCO_3^-. \quad (2)$$

Reaction 2 appears to induce overacidification in the acid jump. We hypothesize that the acid jump in the absence of HCO_3^- is induced by reaction 1, but the acid jump in the presence of HCO_3^- is induced by reactions 1 and 2.

After overacidification, in the presence of HCO_3^-, the pH_i of ATII cells increases rapidly and then gradually; finally, pH_i reaches to the control level. Thus, we found that the pH_i recovery after overacidification during the acid jump consisted of two phases. The pH_i recovery is regulated by various ion transporters and channels, including the plasma membrane Na^+/H^+ exchanger (NHE), the Cl/HCO_3^- exchanger (AE), the Na^+/HCO_3^- cotransporter (NBC), and H^+ channels [3, 4, 8–10]. However, the rapid recovery phase is not eliminated by the inhibition of NHE and NBC. Moreover, in ATII cells, the pH_i recovery, which is induced by NHE, AE, or NBC, is slow and reaches a maximum in 10–15 min [3, 4]. ATII cells have H^+ channels [8], which may maintain the pH_i of ATII cells by facilitating the excretion of H^+. However, little is known about their activities in terms of H^+ excretion.

On the other hand, ATII cells express a large amount of carbonic anhydrase (CA), which processes reaction 3 ($H^+ + HCO_3^- \leftrightarrow CO_2$) [11]. This indicates that HCO_3^- entry may also increase pH_i of ATII cells. In many cell types, Cl^- channels are permeable to HCO_3^- [12, 13]. However, the HCO_3^- permeability of Cl^- channels still remains uncertain in ATII cells.

This study was designed to clarify why HCO_3^- is required in the induction of overacidification in the acid jump, and how ATII cells recover their pH_i after the NH_4^+ pulse removal, particularly in the rapid recovery phase.

Materials and methods

Solutions and chemicals The control solution (solution I) contained (mM): NaCl 121, KCl 4.5, $MgCl_2$ 1, $CaCl_2$ 1.5, $NaHCO_3$ 25, NaHEPES 5, HHEPES 5, and glucose 5. The pH of solution I was adjusted to 7.4 by adding HCl (1 M). For the NH_4^+ pulse (acid loading), 25 mM NaCl of the control solution was replaced with 25 mM NH_4Cl. For high-HCO_3^- concentration experiments, 25 mM NaCl of the control solution was replaced with 25 mM $NaHCO_3$, and the high-HCO_3^- solution was aerated with 90% O_2 and 10% CO_2. The K^+ (Na^+-free) solution contained (mM): KCl 125.5, $MgCl_2$ 1, $CaCl_2$ 1.5, $KHCO_3$ 25, HHEPES 10, and glucose 5, and the pH of the K^+ solution was adjusted to 7.4 by adding KOH (1 M). All HCO_3^--containing solutions were aerated with 95% O_2 and 5% CO_2 at 37°C. In HCO_3^--free experiments, $NaHCO_3^-$ (25 mM) in solution I was replaced with NaCl and aerated with 100% O_2. 5-(*N*-Methyl-*N*-isobutyl)-amiloride (MIA), 5-nitro-2-(3-phenylpropylamino)benzoic acid (NPPB), glybenclamide, bumetanide, acetazolamide, and DNase I were purchased from Sigma (St. Louis, MO), and concanamycin A, baffilomycin A1, 4,4′-diisothiocyanostilbene-2,2′- disulfonic acid-2Na (DIDS), elastase, heparin, and bovine serum albumin (BSA) were purchased from Wako (Osaka, Japan). MIA, DIDS NPPB, concanamycin A, baffilomycin A_1, and glybenclamide were dissolved in dimethyl sulfoxide (DMSO). All the reagents were prepared at their final concentrations immediately before the experiments. The final concentration of DMSO

did not exceed 0.1%, which was previously confirmed to have no effect on cell volume and pH_i [3, 14, 15].

Cell preparations ATII cells were isolated from the lungs of male rats (Slc:Wistar/ST [150–200 g] from SLC, Hamamatsu, Japan) according to previous reports [3, 14–17]. Briefly, the rats were anesthetized by intraperitoneal injection of pentobarbital sodium (60–70 mg/kg) and then heparinized (1,000 units/kg). Their lungs were cleared of blood by perfusion, lavaged, and endotracheally treated with elastase (0.15 mg/ml) and DNase I (0.03 mg/ml) for 30 min at 37°C. After this incubation, both lungs placed in the control solution containing DNase I (0.08 mg/ml) and 3% BSA were minced using fine forceps. The minced tissues were filtered through a nylon mesh with a pore size of 150 μm^2. Isolated cells were washed three times with centrifugation (1,000 rpm for 5 min). The isolated cells were resuspended in the control solution (4°C) and used for experiments within 3 h after preparation.

The surfactant in isolated ATII cells was stained by the modified Papanicolaou method and an immunocytochemical method using SP-D [14, 17, 18]. The results showed that 60–70% of the cells contained surfactant granules as previously reported [14, 16]. Under a differential interference contrast (DIC) microscope, the ATII cells, which have intracellular granules and microvilli, were distinguished from other cells as previously reported [3, 14, 15].

Cell volume measurement Isolated ATII cells were placed on a coverslip precoated with Cell-Tak (Becton Dickinson Labware, Bedford, MA). The coverslip with cells was set in the perfusion chamber that was mounted on the stage of a DIC microscope connected to a video-enhanced contrast system (ARGUS-10, Hamamatsu Photonics, Hamamatsu, Japan), and images were recorded continuously by a video recorder [14, 15]. The volume of the perfusion chamber was approximately 20 μl, and the rate of perfusion was 200 μl/min. Experiments were carried out at 37°C. The focus of the microscope was frequently adjusted to observe the cells at the same focal plane.

To estimate cell volume, the area of a cell was measured by tracing its outline on the video image every 30 s–1 min. The average value obtained from five images measured in the first 2 min was used as the control value (A_0). The relative volume of an ATII cell was expressed as $V/V_0 = (A/A_0)^{1.5}$, where V is the volume, A is the area, and the subscript 0 indicates the control value. Thus, the values of relative cell volume (V/V_0) were normalized to the control value. Volume changes in an ATII cell were estimated, assuming that the volume changed to the same extent in all three dimensions. This method was described in detail previously [14, 15, 19–21]. The values of V/V_0 from four experiments were expressed as means ± SEM.

pH_i measurement Cells were incubated with 5 μM 3′-O-acetyl-2′,7′-bis(carboxyethyl)-4 or 5 carboxyfluorescein diacetoxymethyl ester (BCECF-AM, Dojindo, Kumamoto, Japan) for 30 min at room temperature (22–24°C) in solution I containing 2% BSA and then washed three times with solution I containing 2% BSA. Cells were resuspended and stored in solution I containing 2% BSA at 4°C and placed on a coverslip precoated with neutralized Cell-Tak to allow the cells to adhere firmly to the coverslip. The coverslip with slices was set in a perfusion chamber, which was then mounted on the stage of an inverted microscope (IX70, Olympus, Tokyo, Japan) connected to an image analysis system (ARGUS/HiSCA, Hamamatsu Photonics, Hamamatsu, Japan) [3]. All the experiments were performed at 37°C. The volume of the perfusion chamber was approximately 80 μl, and the rate of perfusion was 500 μl/min. BCECF was excited at 450 and 490 nm, and emission was measured at 530 nm. Fluorescence ratio (F490/F450) was calculated and stored in the image analysis system (ARGUS/HiSCA, Hamamatsu Photonics). The calibration curve for pH_i was obtained from the F490/F450 values of the BCECF-loaded cells, which were perfused with solution II containing nigericin (10 μg/ml). The pH of solution II was set at 6.6, 7.0, 7.2, 7.4, or 7.8. Solution II contained (in mM): KCl 130, NaCl 20, $MgSO_4$ 1, and HEPES 10. One experiment was performed using five to six coverslips from two to three animals, and the pH_i values of six to eight cells from three to six coverslips were expressed as means ± SE. Experiments were performed in pairs of conditions, that is, the NH_4^+ pulse alone (control) and the NH_4^+ pulse with inhibitors or stimulation (experiments), because the recovery rates of intracellular H^+ concentration ($[H^+]_i$) varied in every cell preparation as shown in the results. The results of both "control" and "experiment" are shown in every figure.

Calculation of time constant (τ) To compare pH_i recovery among different experiments, we calculated the time constant (τ) of changes in $[H^+]_i$. The changes in $[H^+]_i$ are expressed in Eq. 3:

$$\left([H^+]_{it} - [H^+]_{i\infty}\right) = \left([H^+]_{i0} - [H^+]_{i\infty}\right) \cdot \exp\left(-t/\tau\right), \quad (3)$$

where "t" is the time, and the subscripts "0" and "∞" indicate $[H^+]_i$ at t=0 and $t = \infty$, respectively.

Eq. 3 can be rewritten as Eq. 4:

$$\ln\left(\left([H^+]_{it} - [H^+]_{i\infty}\right)/\left([H^+]_{i0} - [H^+]_{i\infty}\right)\right) = -1/\tau \cdot t. \quad (4)$$

When "$\ln\left(\left([H^+]_{it} - [H^+]_{i\infty}\right)/\left([H^+]_{i0} - [H^+]_{i\infty}\right)\right)$" is plotted against t (τ plot), the slope shows "$-1/\tau$." In this study, we used $1/\tau$ as an index of pH_i recovery rate. Therefore, we compared the pH_i recovery rate after the NH_4^+ pulse removal among experiments using $1/\tau$ (an index of pH_i recovery rate).

The statistical significance of the differences between the mean values was assessed using Student's t test. Differences were considered significant at $p<0.05$.

Results

Effects of HCO_3^-/CO_2 Figure 1a shows a typical response of the pH_i of rat ATII cells during the NH_4^+ pulse application in the presence of HCO_3^-. The pH_i of ATII cells was 7.4–7.6 (control pH_i). The NH_4^+ pulse addition immediately increased the pH_i (alkali jump), which peaked within 1 min (pH_i=8) and then decreased gradually (pH_i 4 min after the addition of NH_4^+ pulse = 7.9). The NH_4^+ pulse removal immediately decreased the pH_i to 6.9 (acid jump), which is lower than the control pH_i (overacidification). Then, the pH_i initially increased rapidly and then gradually. The pH_i recovered to the control level within 10 min (Fig. 1a).

However, in the absence of HCO_3^-, the NH_4^+ pulse addition induced an alkali jump, but there was no gradual pH_i decrease. Then, the NH_4^+ pulse removal induced the acid jump, but there was no overacidification (Fig. 1b).

The effects of HCO_3^--free solution were examined. The removal of HCO_3^- induced an alkali jump, and the pH_i immediately plateaued. The pH_is of ATII cells before and 4 min after HCO_3^- removal were 7.35 and 7.56, respectively. Then, the addition of 25 mM HCO_3^- induced an acid jump with a small overacidification, and pH_i increased gradually to the control level (Fig. 1c). Thus, the addition of HCO_3^-/CO_2 itself induced overacidification during the acid jump via reaction 3.

We used an inhibitor of CA, 100 μM acetazolamide, to examine the effects of reaction 3 on overacidification during the acid jump. Acetazolamide (100 μM) decreased the extent of overacidification during the acid jump, although it did not affect the alkali jump (Fig. 1d).

Effects of MIA and DIDS MIA (10 μM) and DIDS (200 μM) was used to inhibit NHE and NBC, respectively. Because H^+ extrusion via NHE and HCO_3^- entry via NBC may affect the alkali and acid jumps. MIA and DIDS,

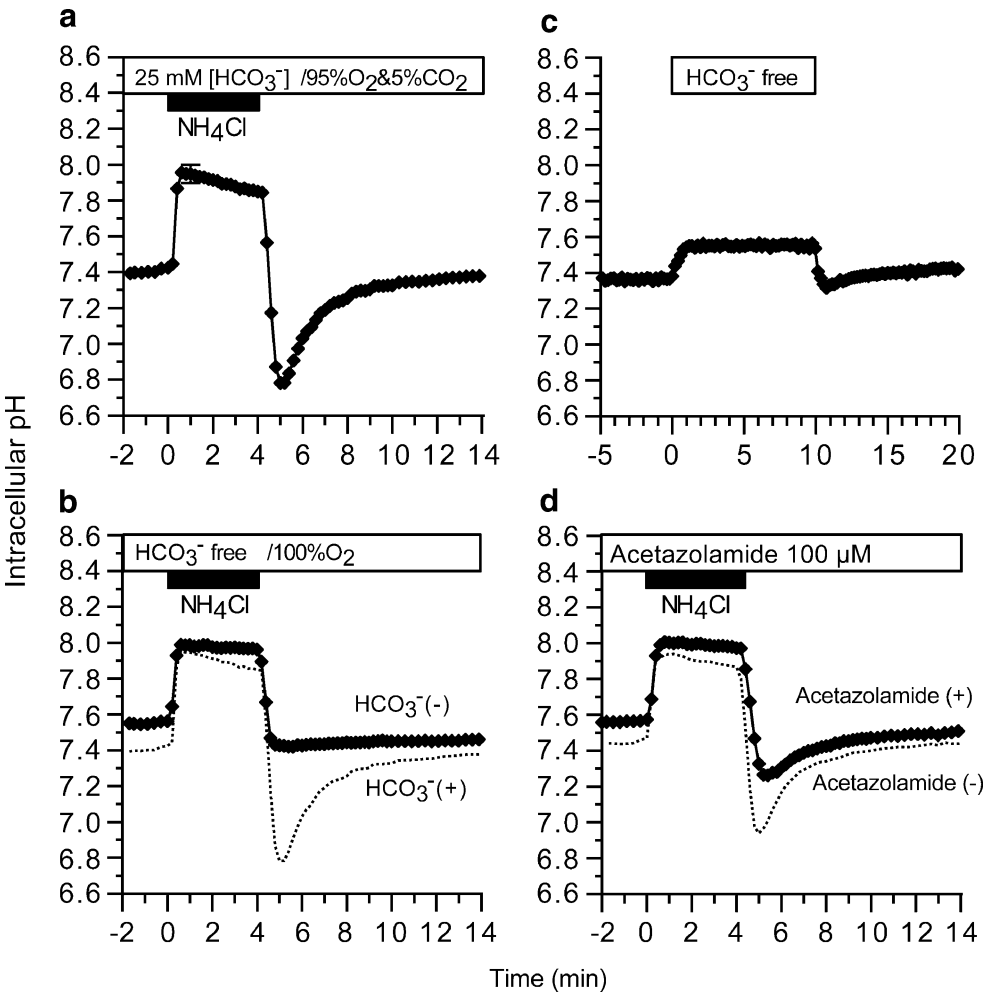

Fig. 1 Changes in pH_i induced by NH_4^+ pulse. **a** HCO_3^--containing condition. The addition of the NH_4^+ pulse induced an alkali jump followed by a gradual decrease in pH_i. The removal of the NH_4^+ pulse induced an acid jump with overacidification. Then, pH_i initially increased rapidly and then gradually to the control level. **b** HCO_3^--free condition. The addition of the NH_4^+ pulse induced an alkali jump, and pH_i was maintained without any gradual decrease. The removal of the NH_4^+ pulse induced an acid jump. The minimum pH_i in the acid jump was slightly lower than the control pH_i. Then, pH_i returned to the control level. **c** Effects of switching to HCO_3^--free solution or control (HCO_3^--containing) solution on pH_i. The switch from the control solution to a HCO_3^--free solution increased pH_i (the alkali jump), whereas the switch to the control solution decreased it (acid jump). **d** Effects of acetazolamide (100 μM). Acetazolamide (100 μM) decreased the extent of overacidification in the acid jump

however, had no effects on the alkali and acid jumps, although they decreased the final pH_i after NH_4^+ pulse removal (Fig. 2a,b).

Effects of bumetanide, NPPB, and glybenclamide The effects of NH_4^+ and Cl^- entry via NKCC on the alkali and acid jumps were examined. To inhibit NKCC, bumetanide (20 μM) was used. Bumetanide (20 μM) did not affect the control pH_i; however, it decreased the extents of both alkaline jump and acid jump. The peak pH_is were 7.9 during the alkali jump and 7.0 during the acid jump in bumetanide-treated ATII cells (Fig. 3a); whereas they were 8 and 6.9 in nonbumetanide-treated cells.

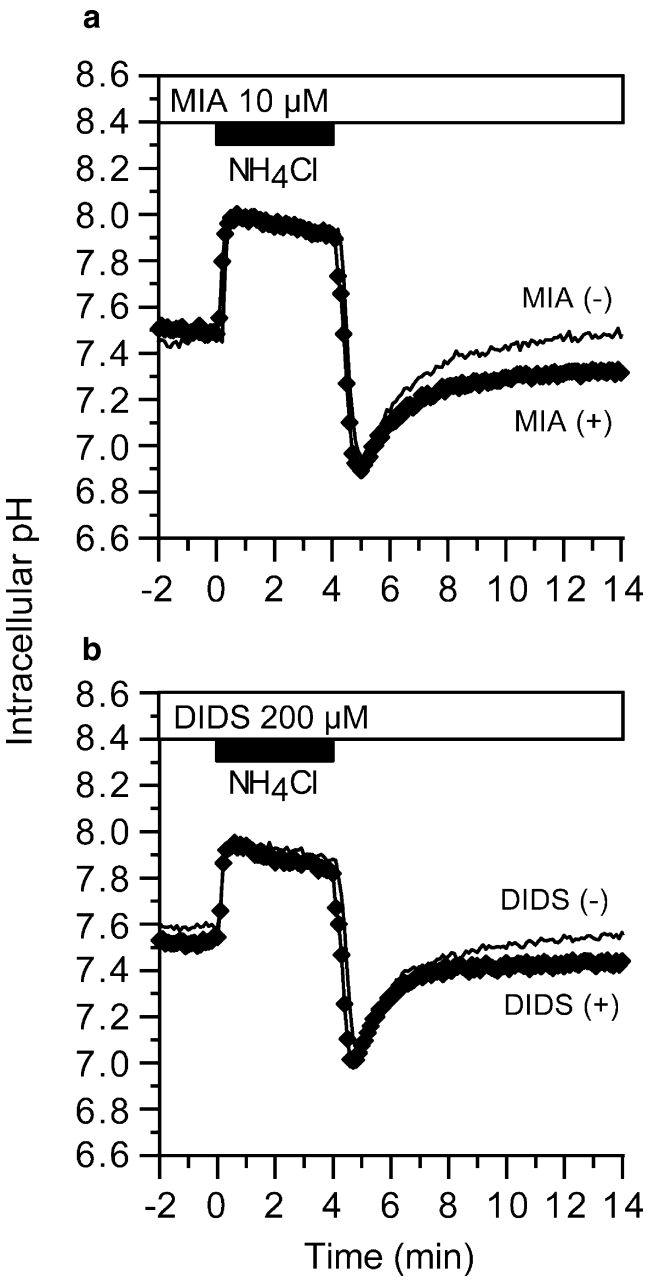

Fig. 2 Effects of MIA and DIDS. **a** MIA (10 μM); **b** DIDS (200 μM). MIA and DIDS did not affect the alkali and acid jumps. After the overacidification, however, they suppressed the gradual pH_i recovery but not the rapid recovery

NPPB and glybenclamide were used to inhibit HCO_3^- entry via Cl^- channels, because HCO_3^- enters the cell via Cl^- channels in many cell types. Both Cl^-channel blockers did not affect the alkali jump; however, they decreased the extent of overacidification during the acid jump (Fig. 3b,c).

The results are summarized in Fig. 4. The extents of the alkali jump were decreased by bumetanide, similar to that induced by the HCO_3^--free solution, and the extent of overacidification during the acid jump was decreased by acetazolamide, bumetanide, NPPB, and glybenclamide. The further addition of NPPB did not enhance decreases in the extent of alkali jump or acid jump induced by bumetanide.

These observations indicates that NH_4^+ entry via NKCC, HCO_3^- entry via Cl^- channels, and CA activity are suggested to be essential to induce overacidification during the acid jump.

pH_i recovery after overacidification After overacidification during the acid jump, pH_i initially increased rapidly and then gradually (Fig. 5a). To analyze the pH_i recovery, the τ plot was used (Fig. 5b). The τ plot showed that the pH_i recovery after overacidification during the acid jump consisted of two phases: a rapid recovery (the first phase within 2 min after the NH_4^+ pulse) followed by a slow recovery (the second phase 3–10 min after the NH_4^+ pulse removal). The regression line of the first phase (labeled "1") was calculated from the values taken within 0–2 min and that of the second phase (labeled "2") was calculated from the values obtained within 3–10 min (Fig. 5b). The index of pH_i recovery rate in the first phase ($1/\tau_1$) was 0.30/min and that of the second phase ($1/\tau_2$) was 0.10/min. The values of $1/\tau_1$ were within the range from 0.3 to 0.4/min, and those of $1/\tau_2$ were from 0.07 to 0.12/min in the control experiments.

Effects of MIA, DIDS, and concanamycin A To examine the effects of NHE and NBC on the pH_i recovery after overacidification during the acid jump, MIA, and DIDS were used. Figure 5c shows the effects of MIA (10 μM). As shown in Fig. 2a, MIA decreased the final pH_i after the NH_4^+ pulse removal. The results of control experiments (panel A) were replotted in panel C (labeled "Control"). The τ plot showed that MIA decreased $1/\tau_2$ but not $1/\tau_1$ (Fig. 5d,e). DIDS (200 μM) also induced similar pH_i changes during the NH_4^+ pulse application, as shown in Fig. 2b. The τ plot also showed that DIDS decreased $1/\tau_2$ (Fig. 5f). Thus, NHE and NBC are suggested to maintain the second phase but not the first phase.

To inhibit H^+ uptake into granules via vacuolar H^+-ATPase, the effects of concanamycin A (5 μM, an inhibitor

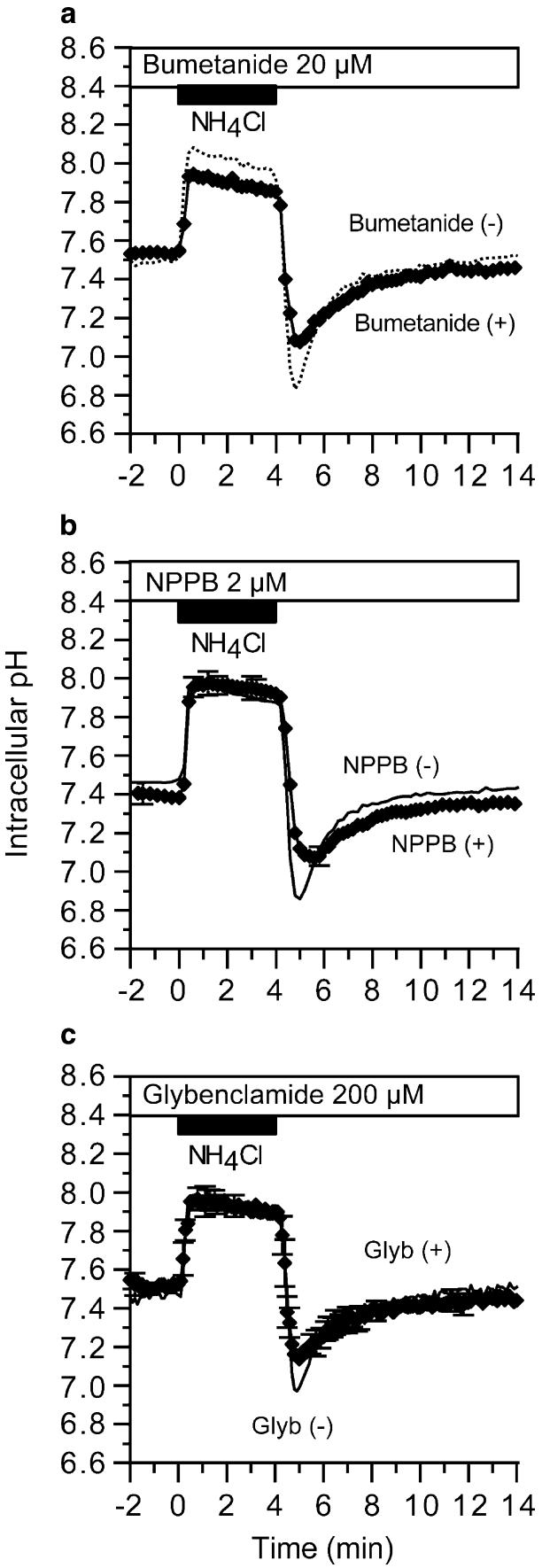

◀ **Fig. 3** Effects of inhibitors of NKCC and Cl^- channel blockers. **a** Bumetanide (20 μM) decreased the extents of the alkali and acid jumps. **b** and **c** NPPB (2 μM) and glybenclamide (200 μM) decreased the extent of overacidification during the acid jump but not changes in pH_i during the alkali jump

of vacuolar H^+-ATPase) were examined. Concanamycin A did not affect pH_i responses induced by the NH_4^+ pulse application (data not shown). Similar results were obtained with baffilomycin A_1 (1 μM).

Effects of Cl^- channel blockers HCO_3^- entry increases pH_i via reaction 3, and Cl^- channels are permeable to HCO_3^- in many cell types [12, 13, 22–32]. Effects of Cl^- channel blockers were examined. NPPB (2 μM) suppressed the pH_i recovery after overacidification during the acid jump (Fig. 6a,c) in addition to decreases in the acid jump (Fig. 3b,c). The τ plot shows that NPPB decreased $1/\tau_1$ and $1/\tau_2$ (Fig. 6b,d,e). Similar results were obtained by 200 μM glybenclamide, although it did not decrease $1/\tau_2$ (Fig. 6f). This suggests that HCO_3^- entry via Cl^- channels maintains the first phase.

Effects of high $\left[HCO_3^-\right]_o$ If HCO_3^- entry via Cl^- channels maintains the first phase, a high extracellular HCO_3^- concentration $\left(\left[HCO_3^-\right]_o\right)$, such as 50 mM, accelerates the first phase because a high $\left[HCO_3^-\right]_o$ increases the driving force for HCO_3^- entry. The control experiments $\left(\left[HCO_3^-\right]_o = 25\ \text{mM}\right)$ were shown in Fig. 7a,b. An increase in $\left[HCO_3^-\right]_o$ (50 mM) accelerated pH_i recoveries during the first and the second phases (Fig. 7c,d). The results ($1/\tau_1$ and $1/\tau_2$ were summarized in Fig. 7e. The acceleration of the first phase ($1/\tau_1$) was inhibited by NPPB (2 μM) and that of the second phase ($1/\tau_2$) was inhibited by DIDS (200 μM; Fig. 7f). Thus, an increase in $\left[HCO_3^-\right]_o$ appears to enhance HCO_3^- entry via Cl^- channels in the first phase and HCO_3^- entry via NBC in the second phases.

Effects of Na^+-free solution and amiloride To examine the driving force for HCO_3^- entry via Cl^- channels, extracellular Na^+ was replaced with K^+. In the K^+ solution, the pH_i recovery after overacidification during the acid jump was consisted of only the slow first phase, that is, the K^+ solution eliminated the second phase (Fig. 8c–e). Thus, the K^+ solution did not eliminate the first phase, although the rate of the first phase was slow compared with that in the control solution. In the K^+ solution ($[K^+]_o$ = 150 mM), the membrane potential depolarizes over an equilibrium potential of Cl^-, which induces K^+ influx into cells. Under this depolarized membrane potential, HCO_3^- appears to enter ATII cells after K^+ influx via K^+ channels. On the other hand, an Na^+-free condition inhibited NHE and NBC, which eliminated the second phase. This suggests that Na^+ entry via Na^+ channels plays an important role for the HCO_3^- entry in the first phase

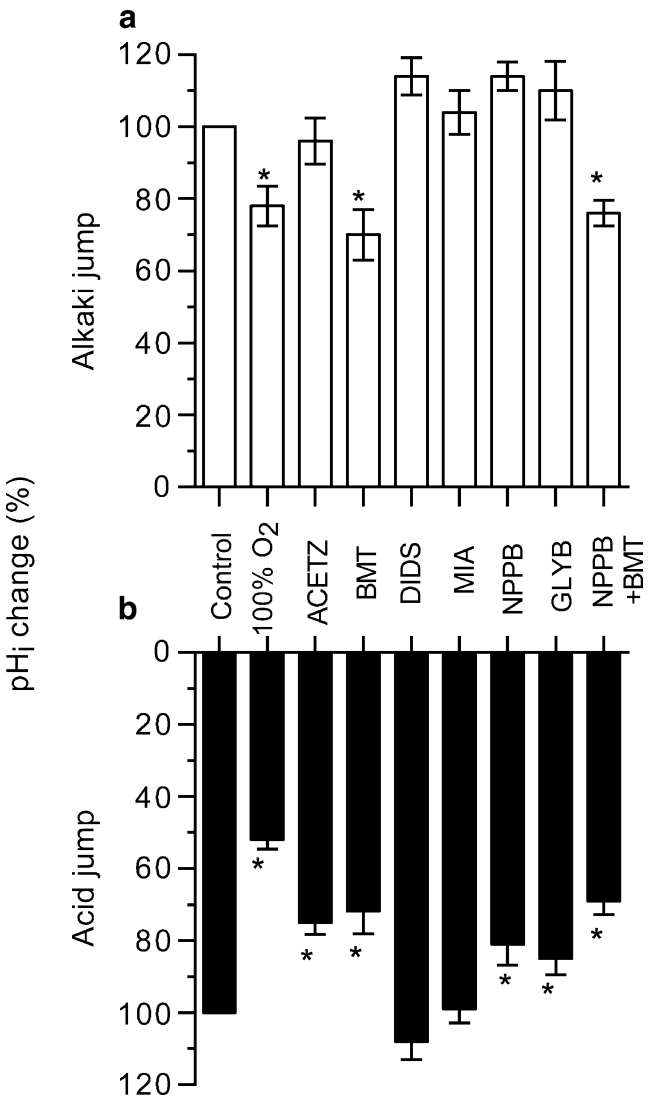

Fig. 4 pH_i changes (%) in alkali (**a**) and acid jumps (**b**). The extents of the alkali jump were decreased by 100% O_2, bumetanide, and both bumetanide and NPPB, and those of the acid jump were decreased by 100% O_2, acetazolamide, bumetanide, NPPB, and glybenclamide

and Na^+-dependent ion transporters (NHE and NBC) for H^+ extrusion and HCO_3^- entry in the second phase.

If HCO_3^- entry is maintained by Na^+ influx via channels, amiloride may inhibit the first phase. The effects of amiloride (1 μM) were examined (Fig. 9). Amiloride (1 μM) inhibited the first phase but not the second phase. Similar results were obtained for benzamil (an inhibitor of Na^+ channels). Thus, the inhibition of Na^+ channels suppressed the first phase but not the second phase. Experiments of K^+ solution and Na^+ channel blockers indicate that the driving force for HCO_3^- entry is maintained by Na^+ entry via Na^+ channels.

The pH_i recovery rates ($1/\tau$) in the first and the second phases were summarized in Fig. 10. The pH_i recovery rates were normalized by the control value in each experiment. In the first phase, Cl^- channel blockers (NPPB and glybenclamide), Na^+ channel blocker (amiloride), and K^+ solution significantly decreased $1/\tau_1$. On the other hand, in the second phase, MIA, DIDS, and K^+ solution decreased $1/\tau_2$ but not glybenclamide and amiloride. NPPB also decreased $1/\tau_2$. The high $\left[HCO_3^-\right]_o$ (50 mM) enhanced both $1/\tau_1$ and $1/\tau_2$. The enhancements of $1/\tau_1$ and $1/\tau_2$ were inhibited by 2 μM NPPB and 200 μM DIDS, respectively (Fig. 7f).

Changes in cell volume To examine the net ion movement, the volume of ATII cell was measured, that is, NH_3 entry, HCO_3^- entry via Cl^- channels, or NH_4^+ entry via NKCC induces cell swelling and, in contrast, NH_3 release or CO_2 release induces cell shrinkage.

In the presence of HCO_3^-, the NH_4^+ pulse addition induced a rapid cell swelling that reached a plateau within 2 min, and in contrast, the NH_4^+ pulse removal induced a rapid and excessive cell shrinkage followed by a cell swelling (Fig. 11a). In the absence of HCO_3^-, the NH_4^+ pulse addition induced cell swelling, similarly in the presence of HCO_3^-. However, after the NH_4^+ pulse removal, the volume of ATII cells decreased and plateaued. The plateau level is higher than the control level (Fig. 11b). Acetazolamide also mimicked the effects of HCO_3^--free solution (Fig. 11c).

The effects of NPPB on cell volume were examined during the NH_4^+ pulse addition. NPPB-enhanced cell swelling induced by the NH_4^+ pulse addition and the excessive cell shrinkage was not noted. The removal of NH_4^+ pulse initially induced a small cell shrinkage followed by a gradual cell shrinkage, and the final volume of ATII cells was higher than that of the control cell volume (Fig. 11d). This suggests that Cl^- release occurred via Cl^- channels, and an inhibition of Cl^- channels may not process NH_4^+ to produce NH_3 via reaction 2. The effects of bumetanide on cell volume were examined. Bumetanide slightly decreased the volume of ATII cells as previously reported [3, 14] and decreased cell swelling induced by the NH_4^+ pulse addition (Fig. 11a,e). The NH_4^+ pulse removal caused the volume of ATII cells to return immediately to the control level (Fig. 11e). Moreover, in the presence of NPPB and bumetanide, the NH_4^+ pulse addition increased the volume of ATII cells and plateaued, and then, the bumetanide removal induced a gradual cell swelling, suggesting that NH_4^+ enters cells via NKCC (Fig. 11f).

Discussion

The NH_4^+ pulse addition increased pH_i (alkali jump) in ATII cells, and the NH_4^+ pulse removal decreased pH_i (acid jump). However, the acid jump after the NH_4^+ pulse removal were different between in the presence and the

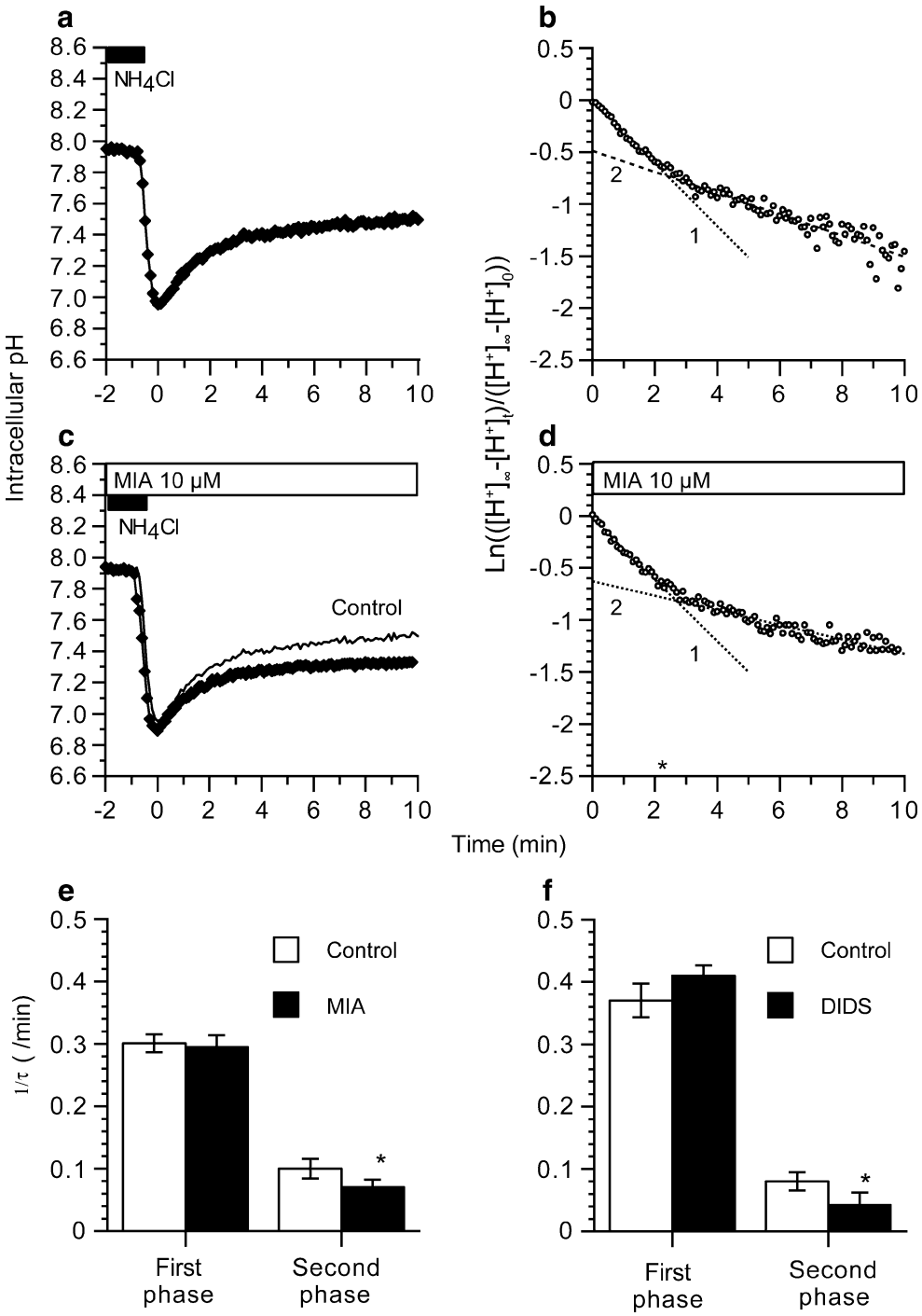

Fig. 5 Effects of MIA (10 μM) and DIDS (200 μM) on recovery of pH_i after the NH_4^+ pulse. **a** pH_i changes in control experiments (n=5). **b** τ plot of control experiments. The pH_i recovery consisted of the first phase followed by the second phase. **c** pH_i changes after the NH_4^+ pulse in the presence of MIA (10 μM; n=5). Cells were treated with MIA (10 μM) for 2 min before the NH_4^+ pulse addition. The *line* marked *Control* shows results of the control experiments. **d** τ plot of the MIA experiments. **e** Effects of MIA (10 μM) on $1/\tau_1$ (first phase) and $1/\tau_2$ (second phase). MIA decreased $1/\tau_2$. **f** Effects of DIDS (200 μM) on $1/\tau_1$ and $1/\tau_2$. DIDS decreased $1/\tau_2$. *Asterisks* indicate $p<0.05$ vs control

absence of HCO_3^-: The NH_4^+ pulse removal induced overacidification in the presence of HCO_3^-, whereas it induced no overacidification in the absence of HCO_3^-.

In the absence of HCO_3^- The NH_4^+ pulse addition accumulates NH_3 because NH_4^+ solution contains a small amount of NH_3 (pK_a=9.25), and NH_3 enters ATII cells and induces reaction 1:

$$NH_3 + H^+ \rightarrow NH_4^+ \left(NH_3 + H_2O \rightarrow NH_4^+ + OH^-\right) \quad (5)$$

This reaction increased pH_i (alkali jump) and intracellular osmolytes, NH_4^+ and OH^- (cell swelling). In contrast, the NH_4^+ pulse removal induces the reversal of reaction 1 (1′):

$$NH_4^+ \rightarrow H^+ + NH_3 \quad (1')$$

This decreased pH_i (acid jump) to the control levels because NH_4^+ produced from NH_3 that entered was reconverted to NH_3, which was then removed from cells.

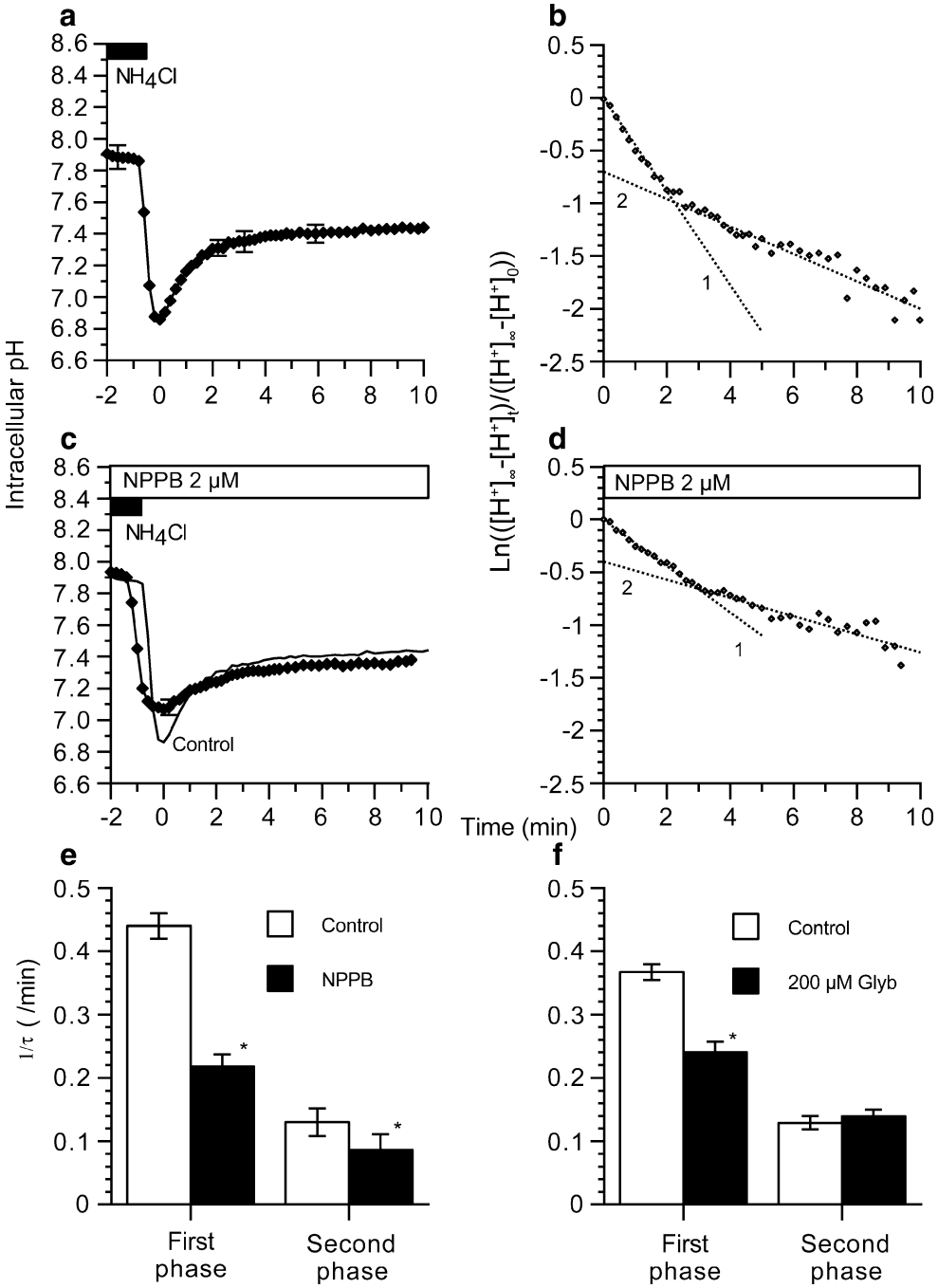

Fig. 6 Effects of NPPB and glybenclamide on pH_i recovery after the NH_4^+ pulse removal. **a** pH_i changes in control experiments (n=5). **b** τ plot of control experiments. **c** pH_i changes after the NH_4^+ pulse removal in the presence of NPPB (2 μM; n=6). The *line* marked *Control* shows results of the control experiments. **d** τ plot in NPPB experiments. **e** Effects of NPPB (2 μM) on $1/\tau_1$ and $1/\tau_2$. NPPB decreased $1/\tau_1$ and $1/\tau_2$. **f** Effects of glybenclamide (200 μM) on $1/\tau_1$ and $1/\tau_2$. Glybenclamide decreased $1/\tau_1$. *Asterisks* indicate $p<0.05$ vs control

The reversal of reaction 1 also decreased intracellular osmolytes, which induced cell shrinkage.

Moreover, the NH_4^+ pulse addition accumulates NH_4^+ and Cl^- via NKCC in many cell types [5–7]. Measurement of ATII cell volume demonstrated that NKCC accumulated NH_4^+ and Cl^- as shown in bumetanide-blockable NPPB-induced cell swelling. However, the NH_4^+ pulse removal did not convert NH_4^+ that entered via NKCC to NH_3, because NH_4^+ is coupled with Cl^- in ATII cells maintaining electroneutrality. Therefore, the volume of ATII cell after the NH_4^+ pulse removal was larger than the control volume. Thus, in the absence of HCO_3^-, the NH_4^+ pulse addition or its removal induced a simple pH_i shift in ATII cells.

In the presence of HCO_3^- The NH_4^+ pulse removal, however, induces three reactions.

$$NH_4^+ \rightarrow H^+ + NH_3 \quad (1')$$

$$NH_4^+ + HCO_3^- \rightarrow NH_3 + H^+ + HCO_3^- \quad (6)$$

$$H^+ + HCO_3^- \rightarrow CO_2 \quad (7)$$

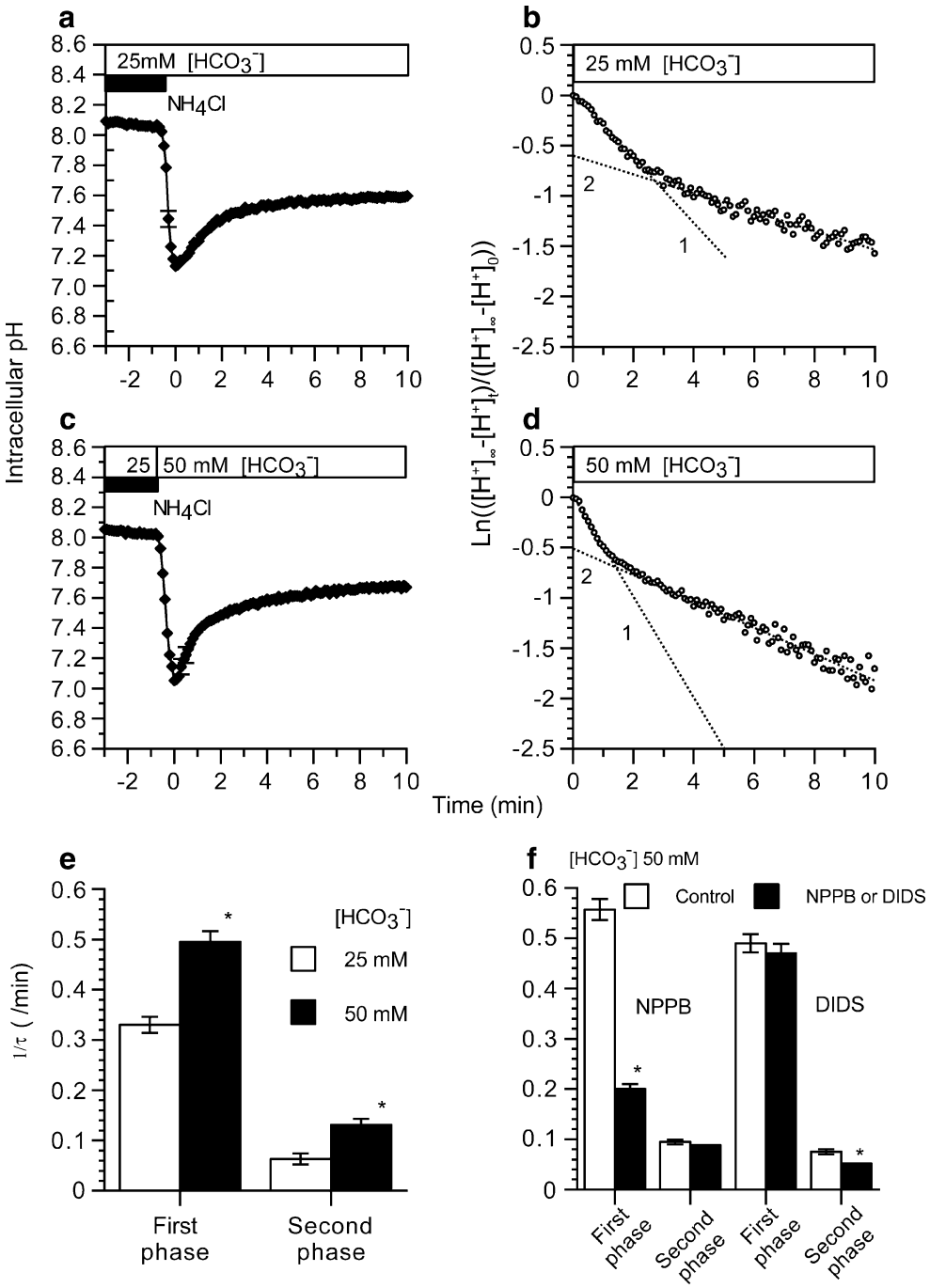

Fig. 7 Effects of high $[HCO_3^-]_o$ (50 mM) on pH_i recovery after the NH_4^+ pulse removal. **a** pH_i changes in control experiments (n=5). **b** τ plot in control experiments. **c** pH_i changes after the NH_4^+ pulse at 50 mM $[HCO_3^-]_o$ (n=5). **d** τ plot at 50 mM $[HCO_3^-]_o$. **e** Effects of 50 mM $[HCO_3^-]_o$ on $1/\tau_1$ and $1/\tau_2$. A high $[HCO_3^-]_o$ (50 mM) increased $1/\tau_1$ and $1/\tau_2$. **f** Effects of NPPB (2 μM) and DIDS (200 μM) on $1/\tau_1$ and $1/\tau_2$ at 50 mM $[HCO_3^-]_o$. *Asterisks* indicate $p<0.05$ vs control

As mentioned above, there are two sources for maintaining the NH_4^+ pool in ATII cells: one is produced from NH_3 that entered via reaction 1, and the other is NH_4^+ entered via NKCC. After the NH_4^+ removal, in the presence of HCO_3^-, NH_4^+ produced via reaction 1 is also reconverted to NH_3 (reaction 1′). Moreover, NH_4^+ that entered via NKCC reacts with HCO_3^- to produce NH_3, H^+, and HCO_3^- (reaction 2) at around 7.0 of pH_i. Then, NH_3 is immediately removed from the cells. Because pK_a values of reactions 1 and 2 are 9.25 and 6.1, respectively, and there is no NH_3 in the extracellular solution. Under this condition, the NH_4^+ pulse removal shifts reaction 2 to the right until intracellular NH_4^+ is absent. This accumulates H^+ and HCO_3^-, which then react to produce CO_2 (reaction 3). Thus, in the presence of HCO_3^-, the NH_4^+ pulse removal produces H^+ via reactions 1′ and 2. The right shift of reaction 2 induced overacidification, and moreover, the reaction 3 following to reaction 2 induced an excessive cell shrinkage during the acid jump.

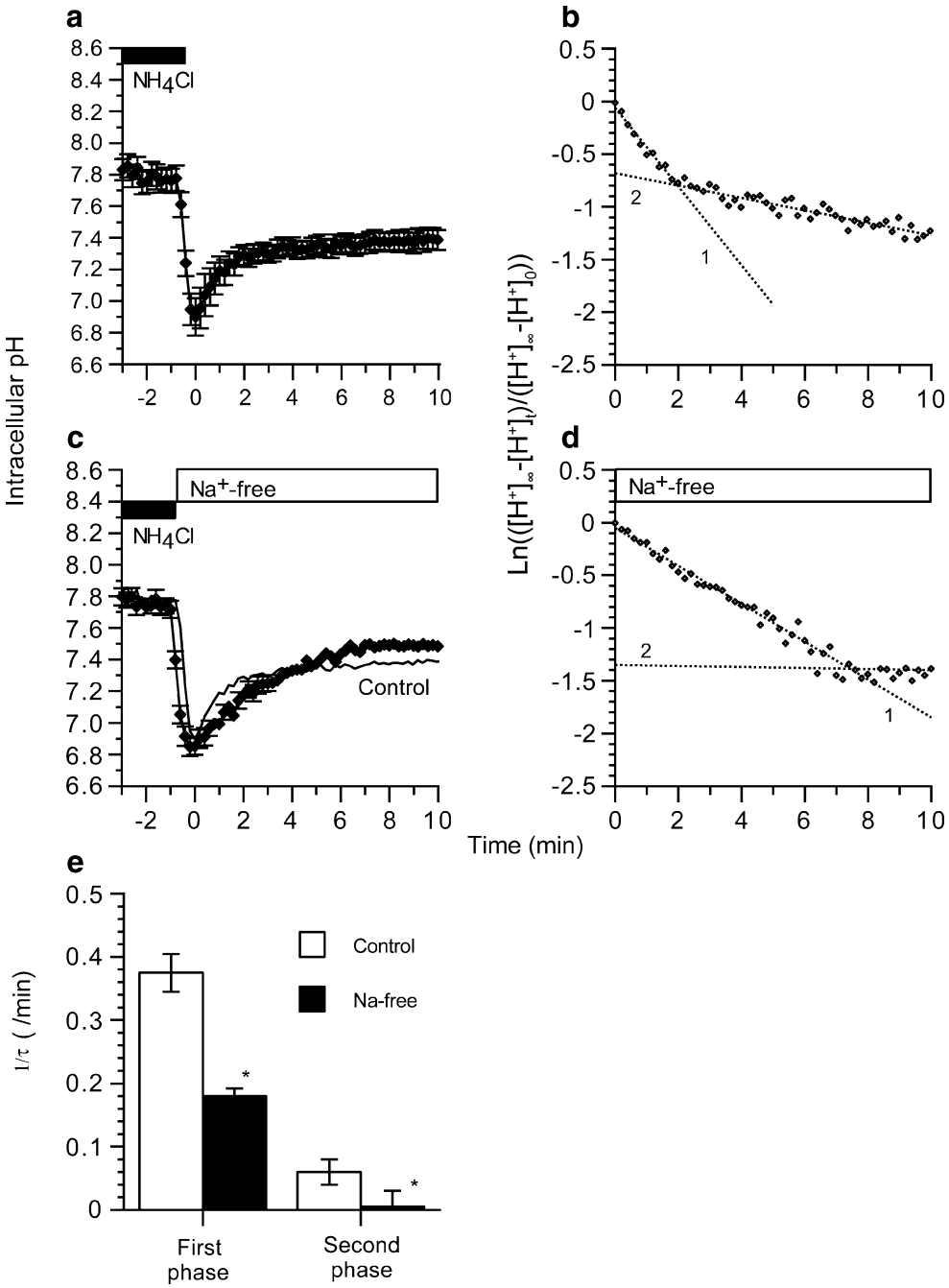

Fig. 8 Effects of Na^+-free solution (K^+ solution). **a** pH_i changes in the control experiments (n=7). **b** τ plot in control experiments. **c** pH_i changes in the K^+ solution experiments (n=7). **d** τ plot in the K^+ solution experiments. In the K^+ solution, only the first phase was detected, and the second phase was not detected. **e** Effects of K^+ solution on $1/\tau_1$ and $1/\tau_2$. *Asterisks* indicate $p<0.05$ vs control

Reactions 1′ and 2 appear to be the same, as HCO_3^- is added in both sides of reaction 1′. However, as discussed above, reaction 2 is different from reaction 1′ because reaction 2 is coupled with reaction 3. The coupling between reactions 2 and 3 was shown by the experiments using acetazolamide (an inhibitor of CA), which mimicked the results of HCO_3^--free solution (marked reduction of overacidification during the acid jump). During inhibition of CA by acetazolamide, the NH_4^+ pulse removal immediately equilibrates reaction 2 because H^+ and HCO_3^- are not removed from cells via reaction 3. This immediate equilibration of reaction 2 made it unable to further react NH_4^+ with HCO_3^-, resulting in only small overacidification. The coupling between two reactions was shown as a gradual decrease in pH_i during the NH_4^+ pulse addition. NH_4^+ accumulated via NKCC reacts with HCO_3^- to produce NH_3, H^+, and HCO_3^- (the right shift of reaction 2), and NH_3 is removed from cells. An accumulation of H^+ and HCO_3^-

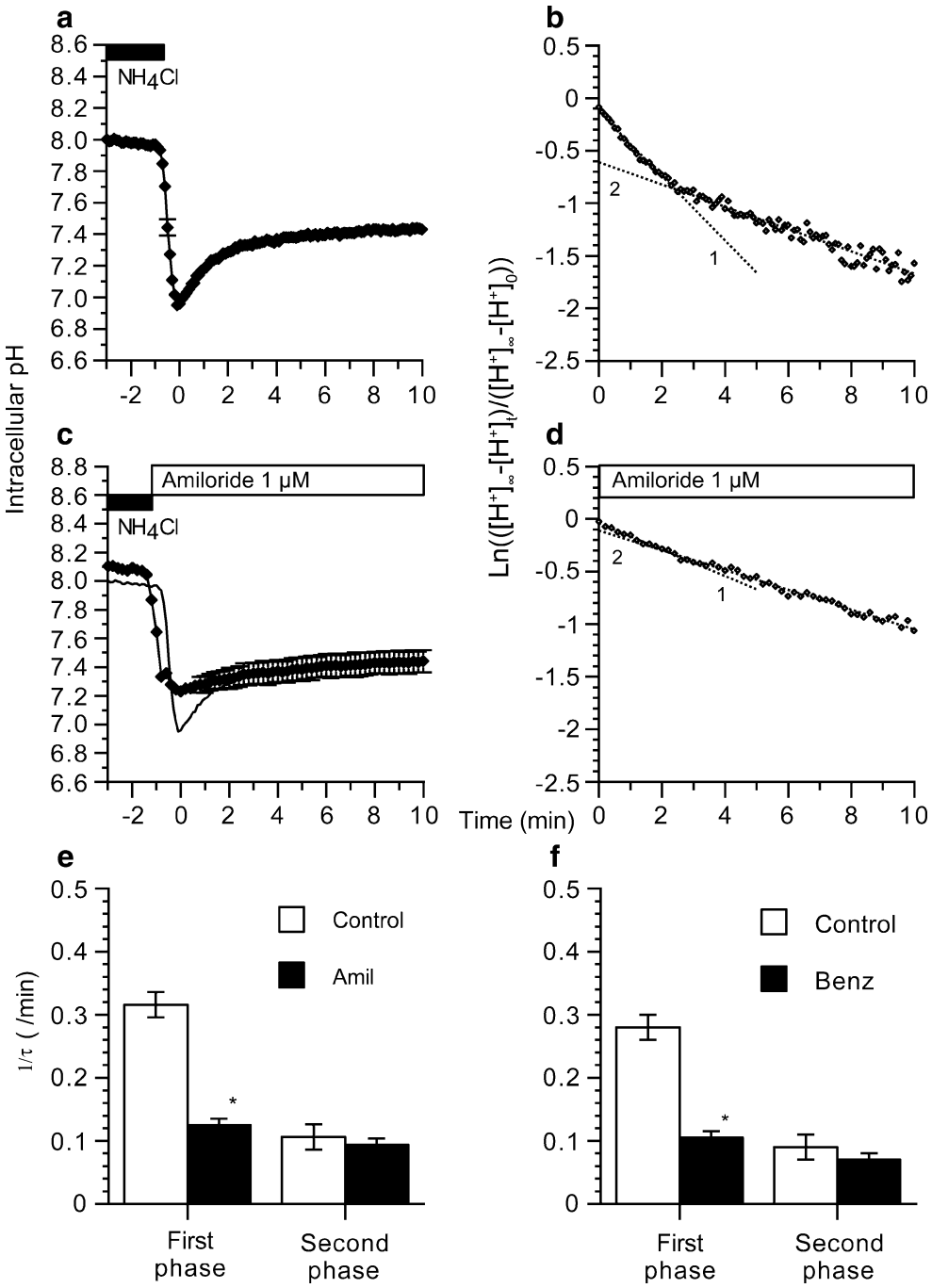

Fig. 9 Effects of Na^+ channel blockers (amiloride and benzamil). **a** pH_i changes in control experiments (n=7). **b** τ plot in the control experiments. **c** pH_i changes after the NH_4^+ pulse removal in the presence of amiloride (1 μM; n=5). The *line* marked *Control* shows results of the control experiments. **d** τ plot in amiloride experiments. **e** Effects of amiloride (1 μM) on $1/\tau_1$ and $1/\tau_2$. Amiloride (1 μM) decreased $1/\tau$ in the first phase but not in the second phase. **f** Effects of benzamil (1 μM) on $1/\tau_1$ and $1/\tau_2$. Benzamil (1 μM) decreased $1/\tau$ in the first phase but not in the second phase. *Asterisks* indicate $p<0.05$ vs control

decreases pH_i gradually during the NH_4^+ pulse addition, and then they are converted to CO_2 via reaction 3, which is removed from cells.

Maintenance of reaction 2 also requires HCO_3^- accumulation. In ATII cells, HCO_3^- enters cells via Cl^- channels coupled with Na^+ entry via amiloride-blockable Na^+ permeable channels, which accumulates HCO_3^- in ATII cells. The details are discussed later. On the other hand, Cl^- leakage via Cl^- channels occurred in ATII cells during the NH_4^+ pulse addition, as shown in NPPB-enhanced cell swelling. Thus, in ATII cells, HCO_3^- entry and Cl^- release occurred. These observations suggest that Cl^- that entered via NKCC is replaced with HCO_3^- in ATII cells during the NH_4^+ pulse addition. This also suggests that Cl^- entry via NKCC is required to maintain HCO_3^- in ATII cells. These indicates that Cl^- channel blockers or NKCC blockers inhibit HCO_3^- accumulation by decreasing HCO_3^- entry or Cl^- entry, respectively, resulting in reduction of overacidification in the acid jump. The present study demonstrated that NPPB, glybenclamide, or bumetanide decreases the extent of

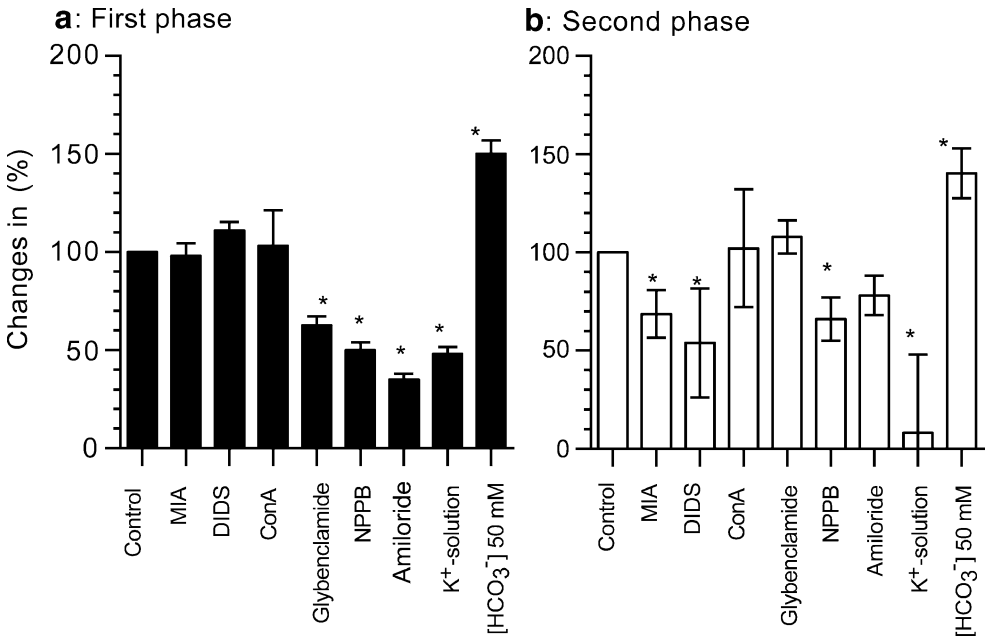

Fig. 10 Changes in $1/\tau$ in experiments. **a** First phase. $1/\tau$ of the first phase was decreased by Cl^- channel blockers, Na^+ channel blockers, and Na^+-free solution and increased by 50 mM $\left[HCO_3^-\right]_o$. **b** Second phase. $1/\tau$ of the first phase was decreased by MIA, DIDS, NPPB, and Na^+-free solution and increased by 50 mM $\left[HCO_3^-\right]_o$

overacidification during the acid jump. Moreover, bumetanide decreased pH_i during the NH_4^+ pulse addition. This pH_i decrease also appears to be caused by HCO_3^- reduction, because a decrease in HCO_3^- shifts reaction 3 to the left (pH_i decrease).

In the absence of HCO_3^-, the removal of the NH_4^+ pulse still induced a slight overacidification [3]. ATII cells produce CO_2 by metabolism. This small amount of CO_2, which reacts with HCO_3^-, leads to NH_3 production via reaction 2, which appears to induce a slight overacidification.

We also examined the effects of a K^+ channel inhibitor, Ba^{2+}, on pH_i changes induced by the NH_4^+ pulse addition and removal; however, Ba^{2+} had no effects on pH_i changes.

pH_i recovery after the NH_4^+ pulse removal In the presence of HCO_3^-, the recovery of pH_i (pH_i increase) after overacidification during the acid jump consisted of two phases: a rapid increase (first phase) followed by a gradual increase (second phase), indicating that ATII cells have at least two mechanisms to increase their pH_i. On the other hand, there are two methods for increasing pH_i in ATII cells: the extrusion of H^+ (such as Na^+/H^+ exchange [NHE] and vacuolar ATPase [V-ATPase]) and the entry of HCO_3^- (Cl^- channels and Na^+/HCO_3^- cotransport [NBC]) [33].

The first phase is inhibited by NPPB and glybenclamide (inhibitors of Cl^- channels) and is accelerated by an increase in $\left[HCO_3^-\right]_o$. However, MIA (an inhibitor of NHE), DIDS (an inhibitor of NBC), or concanamycin A (an inhibitor of V-ATPase) had no effects on the first phase. Cell volume measurements revealed that a rapid cell swelling occurred during the first phase, indicating that ion influx occurred during the first phase. These observations suggest that the first phase is induced by HCO_3^- entry via Cl^- channels not by H^+ extrusion. There was no report showing that HCO_3^- entry via Cl^- channels regulates pH_i after the NH_4^+ pulse removal in ATII cells.

Moreover, amiloride also inhibited the first phase similar to NPPB. This suggests that HCO_3^- entry via Cl^- channels is coupled with Na^+ entry via amiloride-blockable Na^+ channels. Moreover, when extracellular Na^+ is replaced with K^+ (K^+ solution), K^+ entry is occurred instead of Na^+ entry. If HCO_3^- entry via Cl^- channels is coupled with cation influx, K^+ influx via channels should also induce the first phase. The present study clearly demonstrated that the K^+ solution still maintains the first phase after overacidification but not the second phase. These indicate that the driving force for HCO_3^- entry is maintained by Na^+ entry via Na^+ channels.

In ATII cells, the Cl^- channels have already been identified, including cystic fibrosis transmembrane regulator (CFTR) Cl^- channels [28, 34]. Although in CFTR Cl^- channels, the HCO_3^-/Cl^- permeability ratio of CFTR was estimated to be low and ranges from 0.2 to 0.4 [13, 22–27, 29, 30], it has been shown that intracellular signals may change this permeability ratio [31, 32]. HCO_3^- transport via CFTR Cl^- channels in many epithelial cell types, such as fetal lung [34], duodenum [12], distal colon [35], and pancreas [13, 25, 27, 29, 30], has been reported. Moreover,

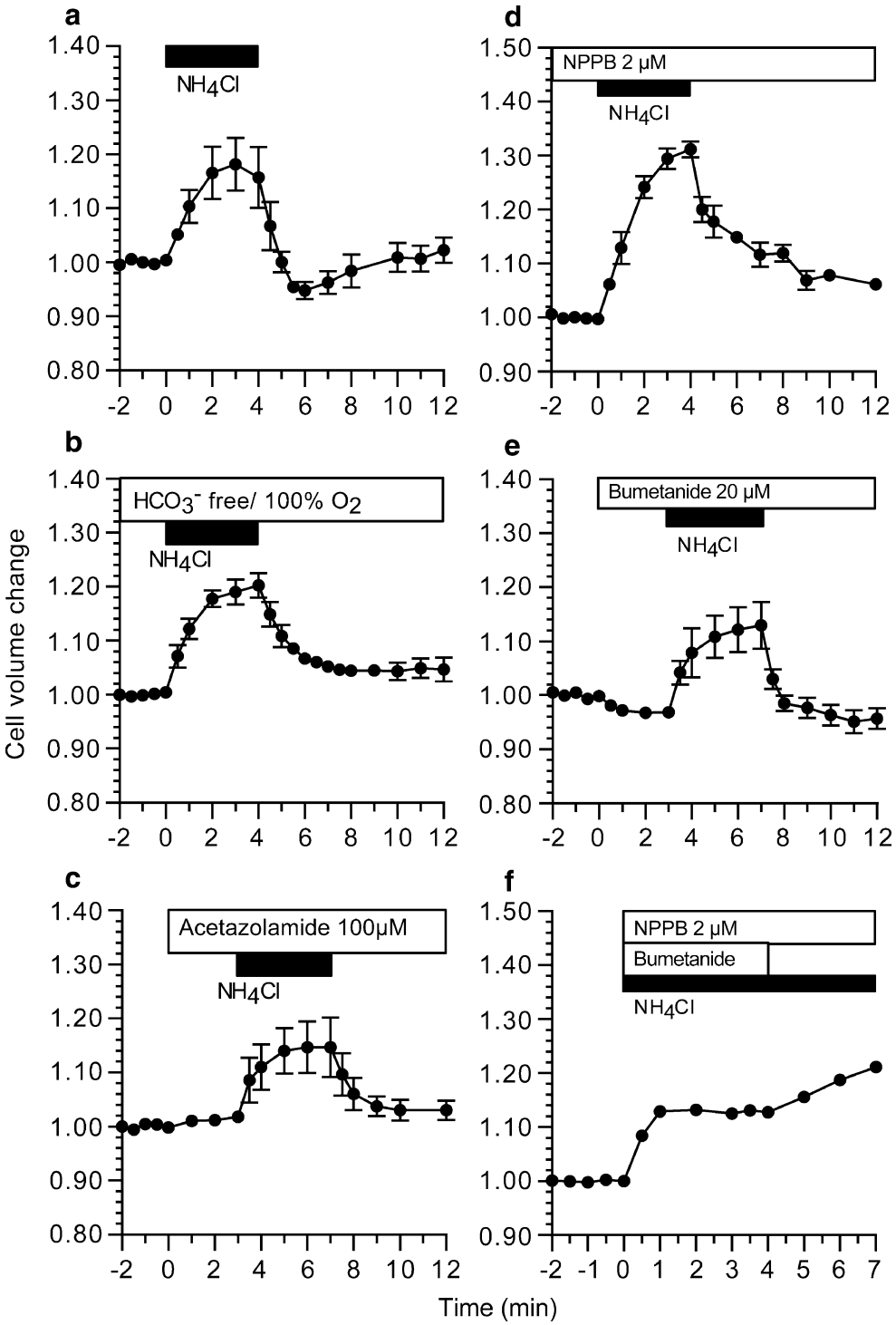

Fig. 11 Cell volume changes during the NH_4^+ pulse addition and its removal. **a** Control experiments. **b** HCO_3^--free experiments. **c** Acetazolamide (100 μM). **d** NPPB (2 μM). NPPB enhanced cell swelling induced by the addition of the NH_4^+ pulse. The removal of the NH_4^+ pulse decreased the volume of ATII cells rapidly and then gradually to the level higher than that before NH_4^+ pulse addition. **e** Bumetanide (20 μM). Bumetanide slightly attenuated cell swelling induced by the addition of the NH_4^+ pulse. No excessive cell shrinkage was detected. **f** Effects of the bumetanide removal during the NPPB addition. The bumetanide removal induced cell swelling gradually

there are some lines of evidence showing that Ca^{2+}-activated Cl^- channels can also transport HCO_3^- in pancreatic duct cells [13, 24, 36]. Thus, in ATII cells, HCO_3^- entry via Cl^- channels appear to be responsible for the first phase.

The second phase was inhibited by MIA (an inhibitor of NHE), DIDS (an inhibitor of DIDS), and an Na^+-free solution and accelerated by a high $\left[HCO_3^-\right]_o$. Murao et al. [3] also showed that a slow pH_i recovery after NH_4^+ pulse removal is inhibited by MIA and DIDS in ATII cells. Moreover, the Na^+-free solution, which inhibits both NHE and NBC, eliminated the second phase. Thus, the second phase was induced by H^+ extrusion via NHE and by HCO_3^- entry via NBC. In the present study, NPPB also decreased the rate of the second phase. NPPB may partially inhibit NHE or NBC.

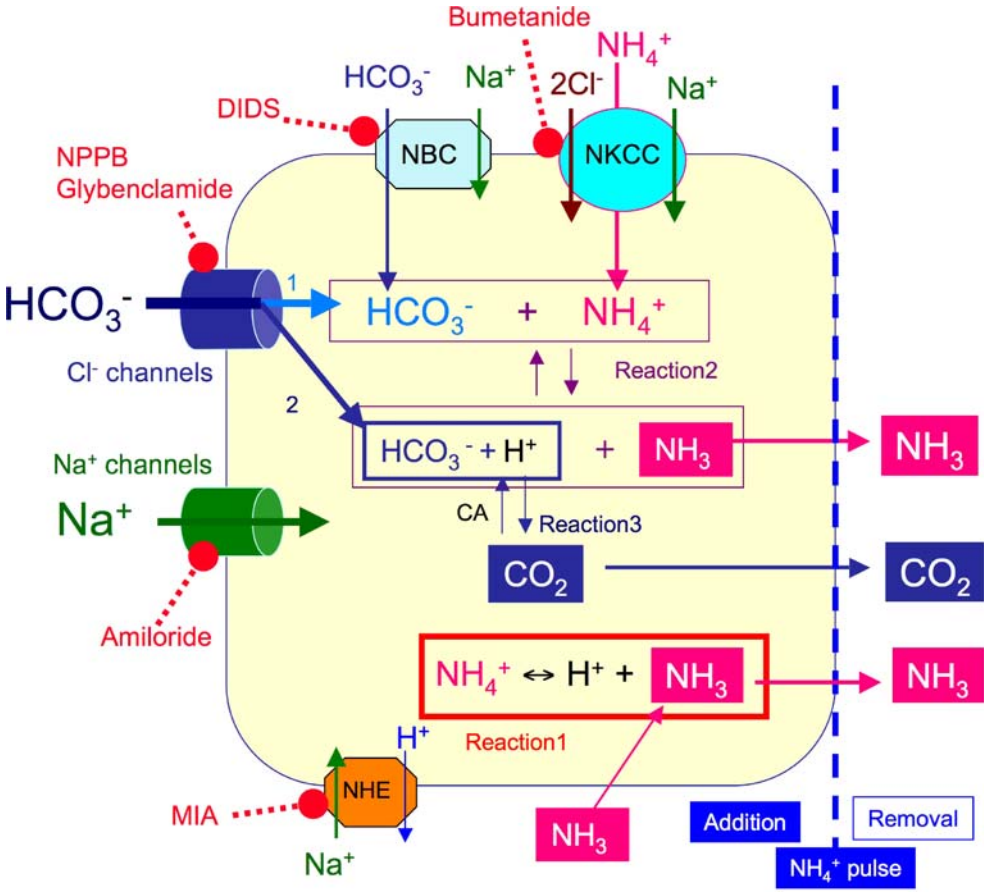

Fig. 12 pH_i regulation in a ATII cell during NH_4^+ pulse addition. Na^+/H^+ exchange (*NHE*), Na^+/HCO_3^- cotransport (*NBC*), $Na^+/K^+/2Cl^-$ cotransport (*NKCC*), and carbonic anhydrase (*CA*). *Label 1* shows HCO_3^- that entered during NH_4^+ pulse addition and overacidification during acid jump after NH_4^+ pulse removal, and *label 2* shows HCO_3^- that entered during pH_i recovery from overacidification during acid jump

NHE and NBC are expressed in the basolateral membrane of ATII cells [9, 10] and are activated by Ca^{2+} or PKC. However, their activation reaches the maximum 5–15 min after the start of their stimulation [3, 10, 11, 37]. This suggests that the activities of NHE and NBC are not sufficient to respond to the first phase, although they are responsible for modulating long-lasting pH_i changes such as second phase.

ATII cells also have H^+ channels [8]. H^+ channels may also play an important role in the pH_i regulation of ATII cells. However, we have only limited knowledge about H^+ channels in ATII cells at present. Further studies are required to clarify the contribution of H^+ channels in the pH_i regulation of ATII cells.

The present study suggests that the lungs may facilitate the removal of NH_3 coupled with CO_2 production. The relationship between breath and blood NH_3 concentration was shown to be nonlinear (see Appendix), suggesting that NH_3 excretion appears to be an active process. In adults, the amount of NH_3 produced by enterobacteria in the gastrointestinal tract is 250 mM/day, most of which (approximately 90%) is metabolized to urea in the liver. The remaining NH_3 (25 mM/day) is believed to be excreted from the kidneys. NH_3 excretion via expiratory air is estimated to be 0.5–1.5 mM/day under a physiological condition because the NH_3 concentrations in expiratory air range from 0.2 to 0.5 μg/dl [38, 39]. However, NH_3 concentration in expiratory air increases five to tenfold with blood NH_3 concentration [38, 39]. Thus, NH_3 excretion via expiratory air may be responsible for an acute overload of NH_3 induced by pathophysiological conditions, such as severe liver cirrhosis. Further studies are required to answer the question, "Is NH_3 excreted from the lungs?"

A schematic diagram of ATII cells is shown in Fig. 12. The NH_4^+ pulse addition induces NH_4^+ accumulation via NKCC and HCO_3^- accumulation via Cl^- channels (labeled "1") in addition to reaction 1 $\left(NH_3 + H^+ \rightarrow NH_4^+\right)$, and reaction 2 $\left(NH_4^+ + HCO_3^- \rightarrow NH_3 + H^+ + HCO_3^-\right)$ reaches an equilibrium. The NH_4^+ pulse removal induces the reversal of reaction 1 and shifts reaction 2 to the right, and NH_3 is removed from ATII cells (overacidification during the acid jump). After that, HCO_3^- entry via Cl^- channels (labelled "2") induces reaction 3 $\left(H^+ + HCO_3^- \rightarrow CO_2\right)$ (pH_i recovery). CO_2 is removed from cells. In conclusion, ATII cells take in NH_4^+ and HCO_3^- via NKCC and Cl^- channels, respectively, and NH_4^+ reacts with HCO_3^- to produce NH_3 and CO_2, and NH_3 and CO_2 is then removed from ATII cells.

Acknowledgment This study was performed as a research project (Nakahari Project) of the Central Research Laboratory in Osaka Medical College and was partly supported by a grant to T. Nakahari from the Japan Science and Technology Agency.

Appendix

Relationship between breath and blood ammonia concentrations

Chikao Shimamoto

The relationship between breath and blood ammonia concentrations was examined in ten healthy volunteers and 15 liver cirrhotic patients who were admitted to the Osaka Medical College Hospital. Patients with hepatic encephalopathy, respiratory disorders, and renal impairment were excluded. Venous blood was collected early in the morning after overnight fasting, and then blood ammonia concentration was measured immediately by direct colorimetric analysis. After blood sampling, expired air was collected. To measure ammonia in expired air, an ammonia electrode method was used [1]. A bag for the modified ^{13}C urea breath test was used for the collection of expired air. After deep breathing, breath was held for 10 s, and then expired air was collected into the bag. Then, an ammonia electrode (Chemical, Tokyo, Japan) was inserted into the bag, and the ammonia concentration in expired air was measured. The reliability of the ammonia electrode method was confirmed in previous reports [1, 2].

This study was approved by the Ethics Review Committee of Osaka Medical College and was conducted according to the guidelines of this committee.

Breath ammonia concentrations were plotted against blood ammonia concentrations. The breath ammonia concentrations were almost constant (approximately 0.3–0.4 ppm) when the blood ammonia concentrations were less than 70 μg/dl. The increment of blood ammonia concentration from 80 to 220 μg/dl increased breath ammonia concentration in a linear relationship, as shown in Fig. 13. A similar relationship between breath and blood ammonia concentrations determined using a sensor tube type-gas assay system was reported [3]. If NH_3 is excreted from blood into the alveolar space by simple diffusion, the relationship between breath and blood ammonia concentrations should show a linear relationship through the origin of the coordinate axes. However, the results show a nonlinear relationship.

Acknowledgment

We thank the patients and healthy volunteers who volunteered to participate in this study.

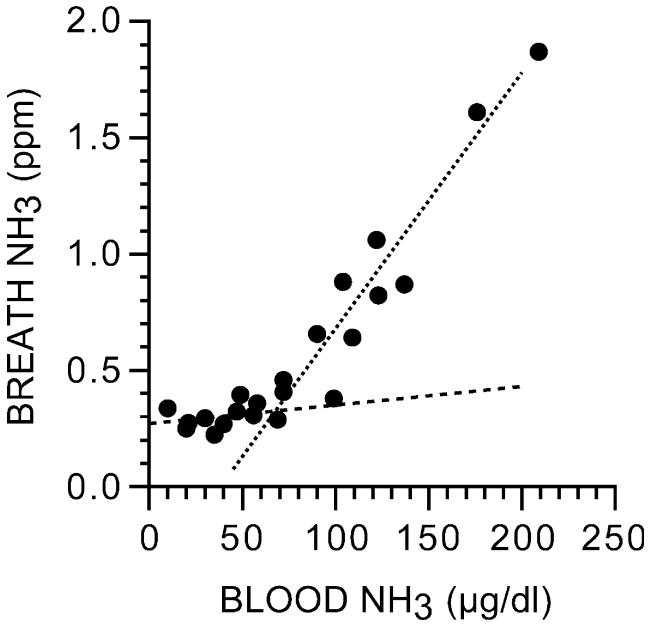

Fig. 13 Relationship between breath and blood ammonia concentrations

References

1. Sutto Z, Conner GE, Salate M (2004) Regulation of human airway ciliary beat frequency by intracellular pH. J Physiol 560:519–532
2. Evans RL, Turner RJ (1997) Upregulation of Na^+-K^+-$2Cl^-$ cotransporter activity in rat parotid acinar cells by muscarinic stimulation. J Physiol 499:351–359
3. Murao H, Shimizu A, Hosoi K, Iwagaki A, Min K-Y, Kishima G, Hanafusa T, Kubota T, Kato M, Yoshida H, Nakahari T (2005) Cell shrinkage evoked by Ca^{2+}-free solution in rat alveolar type II cells: Ca^{2+} regulation of Na^+-H^+ exchange. Exp Physiol 90:203–213
4. Wadsworth S, Wu A-M, Spitzer A, Chander A (1996) Protein kinase C in intracellular pH regulation in alveolar type II cells. Am J Physiol 271:L106–L113
5. Amlal H, Paillard M, Bichara M (1994) Cl^--dependent NH_4^+ transport mechanisms in medullary thick ascending limb cells. Am J Physiol 267(Cell Physiol 36):C1607–C1615
6. Kikeri D, Sun A, Zeidel ML, Hebert SC (1989) Cell membranes impermeable to NH_3. Nature 339:478–480
7. Kinne R, Kinne-Saffran E, Schölermann B, Schütz H (1986) Ammonium transport in medullary thick ascending limb of rabbit kidney: involvement of the Na^+, K^+, Cl(−)-cotransporter. J Membr Biol 94:279–284
8. Cherny VV, Markin VS, DeCoursey TE (1995) The voltage-activated hydrogen ion conductance in rat alveolar epithelial cells is determined by the pH gradient. J Gen Physiol 105:861–896
9. Dudeja PK, Hafez N, Tyagi S, Gailey CA, Toofanfard M, Alrefai WA, Nazir TM, Ramaswamy K, Al-Bazzar FJ (1999) Expression of Na^+/H^+ and Cl/HCO_3^- exchanger isoforms in proximal and distal airways. Am J Physiol 276(Lung Cell Mol Physiol 20): L971–L978

10. Lubman RL, Chao DC, Crandall ED (1995) Basolateral localization of $Na^+ - HCO_3^-$ cotransporter activity in alveolar epithelial cell. Respir Physiol 100:15–24
11. Fleming RE, Moxley MA, Waheed A, Crouch EC, Sly WS, Longmore WJ (1994) Carbonic anhydrase II expression in rat type II pneumocytes. Am J Respir Cell Mol Biol 10:499–505
12. Furukawa O, Hirokawa M, Zhang L, Takeuchi T, Bi LC, Guth PH, Engel E, Akiba Y, Kaunitz JD (2005) Mechanism of augmented duodenal HCO_3^- secretion after elevation of luminar CO_2. Am J Physiol Gasterointest Liver Physiol 288:G557–G563
13. Steward MC, Ishiguro H, Case RM (2005) Mechanism of bicarbonate secretion in the pancreatic duct. Annu Rev Physiol 67:14.1–14.33
14. Hosoi K, Min KY, Shiima C, Hanafusa T, Mori H, Nakahari T (2002) Terbutaline-induced triphasic changes in volume of rat alveolar type II cells: role of cAMP. Jpn J Physiol 52:561–572
15. Hosoi K, Min KY, Iwagaki A, Murao H, Hanafusa T, Shimamoto C, Katsu K, Kato M, Fujiwara S, Nakahari T (2004) Delayed shrinkage triggered by the Na^+-K^+ pump in terbutaline-stimulated rat alveolar type II cells. Exp Physiol 89:373–385
16. Dobbs LG, Geppert EF, Williams MC, Greenleaf RD, Mason RJ (1980) Metabolic properties and ultrastructure of alveolar type II cells isolated with elastase. Biochim Biophys Acta 618:510–523
17. Kikkawa Y, Yoneda K (1974) The type II epithelial cells of the lung. I. Method of isolation. Lab Invest 30:76–84
18. Kasper M, Albrecht S, Grossmann H, Grosser M, Sehuh D, Muller M (1995) Monoclonal antibodies to surfactant protein D: evaluation of immunoreactivity in normal rat lung and in a radiation-induced fibrosis model. Exp Lung Res 21:577–588
19. Nakahari T, Murakami M, Yoshida H, Miyamoto M, Sohma Y, Imai Y (1990) Decrease in rat submandibular acinar cell volume during ACh stimulation. Am J Physiol 258:G878–G886
20. Nakahari T, Marunaka Y (1996) Regulation of cell volume by β_2-adrenergic stimulation in rat fetal distal lung epithelial cells. J Membr Biol 151:91–100
21. Nakahari T, Marunaka Y (1997) β-agonist-induced activation of Na^+ absorption and KCl release in rat fetal distal lung epithelium: a study of cell volume regulation. Exp Physiol 82:521–536
22. Gray MA, Pollard CE, Harris A, Coleman L, Greenwell JR, Argent BE (1990) Anion selectivity and block of the small-conductance chloride channel on pancreatic duct cells. Am J Physiol Cell Physiol 259:C752–C761
23. Gray MA, Plant S, Argent BE (1993) cAMP-regulated whole cell chloride currents in pancreatic duct cells. Am J Physiol Cell Physiol 264:C591–C602
24. Gray MA, Winpenny JP, Verdon B, O'Reilly CM, Argent BE (2002) Properties and role of Ca^{2+}-activated chloride channels in pancreatic duct cells. In: Fuller CM (ed) Calcium-activated chloride channels. Academic, San Diego, pp 231–256
25. Illek B, Tam AWK, Fischer H, Machen TE (1999) Anion selectivity of apical membrane conductance of Calu 3 human airway epithelium. Pfluegers Arch 437:812–822
26. Illek B, Yankaskas JR, Machen TE (1997) cAMP and genistein stimulate HCO_3^- conductance through CFTR in human airway epithelia. Am J Physiol Lung Cell Mol Physiol 272:L752–L761
27. Linsdell P, Tabcharani JA, Rommens JM, Hou YX, Chang XB, Tsui LC, Riordan JR, Hanrahan JW (1997) Permeability of wild-type and mutant cystic fibrosis transmembrane conductance regulator chloride channels to polyatomic anions. J Gen Physiol 110:355–364
28. O'Grady SM, Lee SY (2003) Chloride and potassium channel function in alveolar epithelial cells. Am J Physiol Lung Mol Physiol 284:L689–L700
29. O'Reilly CM, Winpenny JP, Porteous DJ, Dorin JR, Argent BE (2000) Cystic fibrosis transmembrane conductance regulator currents in guinea pig pancreatic duct cells: inhibition by bicarbonate ions. Gastroenterology 118:1187–1196
30. Poulsen JH, Fischer H, Illek B, Machen TE (1994) Bicarbonate conductance and pH regulatory capability of cystic fibrosis transmembrane conductance regulator. Proc Natl Acad Sci USA 91:5340–5344
31. Reddy MM, Quinton PM (2003) Control of dynamic CFTR selectivity by glutamate and ATP in epithelial cells. Nature 423:756–760
32. Shcheynikov N, Kim KH, Kim K-M, Dorwart MR, Ko SBH (2004) Dynamic control of cystic fibrosis transmembrane conductance regulator Cl/HCO_3^- selectivity by external Cl^-. J Biol Chem 279:21857–21865
33. Roos A, Boron WF (1981) Intracellular pH. Physiol Rev 61:296–434
34. Lazrak A, Thome U, Myles C, Ware J, Chen L, Venglarik CJ, Matalon S (2002) cAMP regulation of Cl^- and HCO_3^- secretion across rat fetal distal lung epithelial cells. Am J Physiol Lung Cell Mol Physiol 282:L650–L658
35. Vidyasagar S, Rajendran VM, Binder HJ (2004) Three distinct mechanisms of HCO_3^- secretion in rat distal colon. Am J Physiol Cell Physiol 287:C612–C621
36. Zsembery A, Strazzabosco M, Graf J (2000) Ca^{2+}-activated Cl^- channels can substitute for CFTR in stimulation of pancreatic duct bicarbonate secretion. FASEB J 14:2345–2356
37. Lubman RL, Crandall ED (1992) Regulation of intracellular pH in alveolar epithelial cells. Am J Physiol 262(Lung Cell Mol Physiol 6): L1–L14
38. Shimamoto C, Hirata I, Katsu K (2000) Breath and blood ammonia in liver cirrhosis. Hepato-Gastroenterol 47:443–445
39. Wakabayashi H, Kuwabara Y, Murata H, Kobashi K, Watanabe A (1997) Measurement of the expiratory ammonia concentration and its clinical significance. Metab Brain Dis 12:161–169

Further Readings

1. Shimamoto C, Hirata I, Katsu K (2000) Breath and blood ammonia in liver cirrhosis. Hepato-Gastroenterol 47:443–445
2. Kearney DJ, Hubbard T, Putnam D (2002) Breath ammonia measurement in helicobacter pylori infection. Dig Dis Sci 47:2523–2530
3. Wakabayashi H, Kuwabara Y, Murata H, Kobashi K, Watanabe A (1997) Measurement of the expiratory ammonia concentration and its clinical significance. Metab Brain Dis 12:161–169